

## CHAPTER 3

### MATERIALS AND METHODS

#### 3.1 Methodology

##### 3.1.1 Moisture measurement system design

As aforementioned, one of the most popular indirect methods for moisture measurement is by using the electrical properties including resistance and capacitance. As for electrical capacitance, it is dependent on the dielectric properties of the material inserted between the plates of a capacitor, i.e.,

$$C = \frac{\varepsilon_0 K A}{d}, \quad (3.1)$$

where

$C$  : Capacitance, (pF)

$A$  : Surface area of the plates, (m<sup>2</sup>)

$d$  : Distance between the plates, (m)

$\varepsilon_0$  : Permittivity in vacuum ( $8.854 \times 10^{-12}$  F/m)

$K$  : Dielectric constant of the dielectric material.

This research proposes an original method to measure the moisture content of dried longan aril. This measurement is obtained using five components: a direct-current power supply circuit, an oscillator circuit, a frequency divider circuit, a computation unit and an LCD display circuit. The diagram of the overall system is shown in figure 3.1.

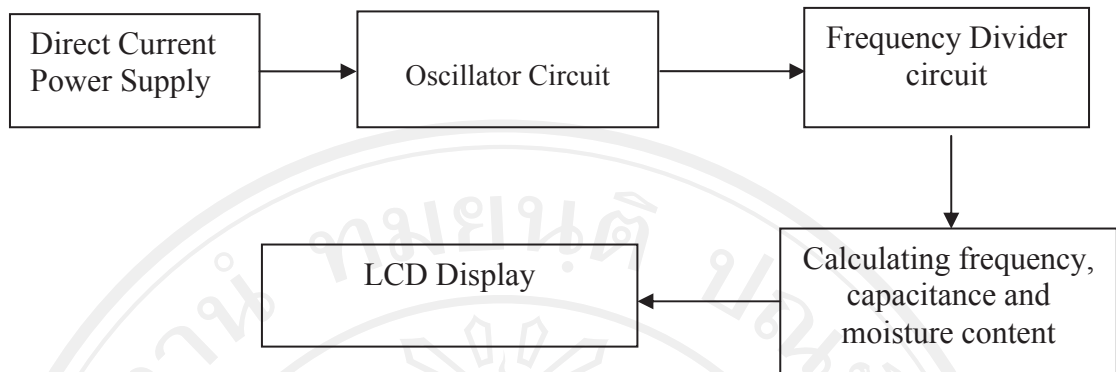


**Figure 3.1 Diagram of overall moisture measurement system**

The moisture measurement system works with a direct current power supply. This system used the direct-current voltages ( $V_{dc}$ ) of +5 volts, +10 volts and 2 amperes of current on average. Therefore, household electricity will be transformed from the alternating-current voltage ( $V_{ac}$ ) of 220 volts to  $V_{dc}$  of +5 and +10 volts. The diagram in figure 3.2 shows the four steps by which the alternating current is converted into a direct current.

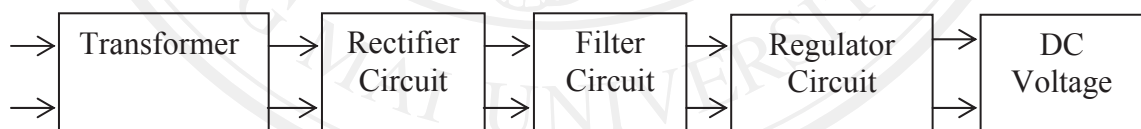


**Figure 3.2 Direct-current power supply of the moisture measurement system**

### 3.1.2 Transformer

The transformer uses a power supply of 220 volts for the primary and a power supply of 12 volts for the secondary. The maximum current of the transformer is limited to 2 amperes. The main reason this particular specification of transformer was selected comes from the need to use in conjunction with a bridge rectifier circuit. The voltage approximation can be computed from

$$\bar{V}_{dc} = \frac{2V_p}{\pi} = \frac{2(\sqrt{2}V_{dc})}{\pi} = \frac{2(\sqrt{2} \times 12)}{\pi} = 10.80 \text{ volts}, \quad (3.2)$$

where  $V_p$  is the peak voltage which has the value of  $\sqrt{2}V_{ac}$ . In the actual testing though, the alternating current of the secondary transformer may be above 12 volts, this results in a  $V_{dc}$  of more than 10.80 volts. From the experiments, we found that  $V_{dc}$  could be up 8 to 16.20 volts. We will use this value as the maximum  $V_{dc}$  in this research.

### 3.1.3 Capacitor filter circuit

After the alternating current is rectified by the rectifier circuit, a resulting direct current may still consist of the alternating current components. Therefore, to eliminate the alternating current components from a direct current, a filter circuit was inserted between the rectifier circuit and the regulator circuit. The filter is based on the capacitor filter circuit. Bogart (1993) found that the percent ripple is

$$r = \frac{V_{rms}}{V_{dc}} = \frac{1}{2\sqrt{3}f_r R_L C} \times 100\%, \quad (3.3)$$

Where

$f_r$  : Second harmonic of household frequency ( $2 \times 50$  Hz)

$R_L$  : Load resistance (50 ohms)

In this research, we set the percent ripple to 2 %. The capacitor in the filter circuit can therefore be derived from

$$C = \frac{1}{2\sqrt{3} \times 100 \times 50 \times 0.02} = 2886.75 \mu F. \quad (3.4)$$

According to capacitors available in the market, we chose  $C = 4,700$  microfarads for our system.

### 3.1.4 Regulator circuit

The most important issue of the voltage power supply circuit is on the stability of the circuit to maintain the current and voltage after supplied to all circuits. A series regulator circuit was selected in this proposed system. The output voltage is computed from

$$V_o = \left(1 + \frac{R_2}{R_1}\right) V_Z, \quad (3.5)$$

Where

$V_o$ : Output voltage, and  
 $V_Z$ : Breakdown voltage of a Zener diode (3.3 volt for the Zener diode used in the proposed system)

The system used a direct current with +5 volts for a microprocessor and +10 volts for an oscillator circuit (ICL 8038). The output voltage of the regulator circuit can be calculated by choosing the resistor  $R_1 = 1 \text{ k}\Omega$  and then determining the value of the resistance of  $R_2$  by using equation (3.5). After that, the resistor  $R_3$  is obtained by considering the maximum rating of the Zener diode current and voltage. All of the components are computed as follows:

$$V_o = \left(1 + \frac{1000}{R_1}\right) \times 3.3 = 16.20 \text{ volts.} \quad (3.6)$$

Solving equation (3.6) yields  $R_2 = 255.8$  ohms. Given  $I_z = 30$  milliamperes and  $V_{in} = 16.20$  volts, we get

$$R_3 = \frac{V_{in} - V_Z}{I_z} = \frac{16.20 - 3.3}{30 \times 10^{-3}} = 430 \Omega. \quad (3.7)$$

In this research, we chose  $R_3 = 470$  ohms and chose a 10 kilo-ohms variable resistor for  $R_2$ . The circuit diagram of the regulator circuit designed for the proposed moisture measurement system is shown in figure 3.3

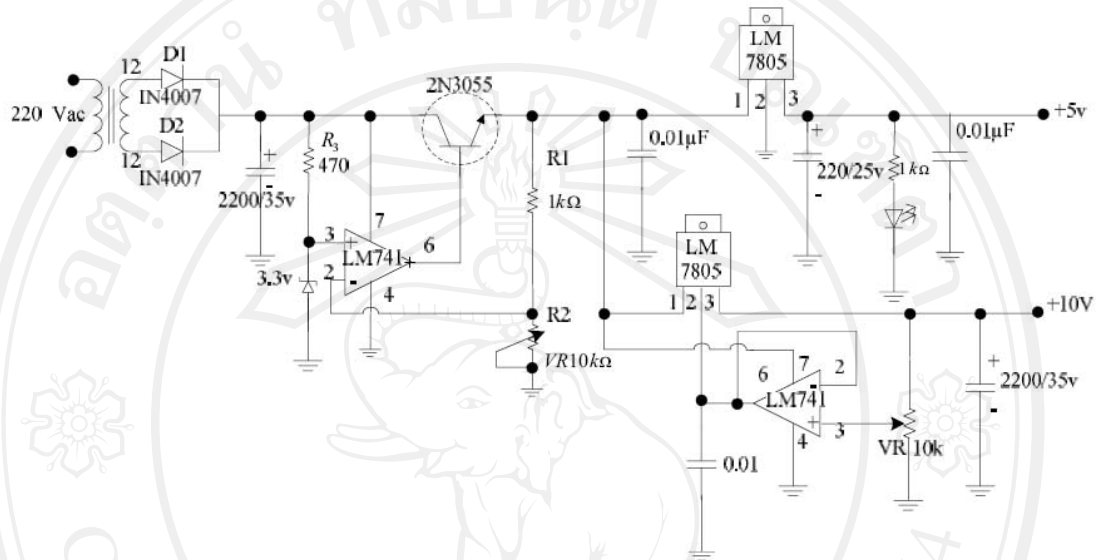


**Figure 3.3 Regulator circuit in the moisture measurement system**

### 3.1.5 Oscillator circuit operations

The operation of the moisture measurement system is based on the principle of the waveform generation and measuring technique. An oscillator circuit was applied to generate a waveform for this system. In this research, we chose an ICL8038 integrated circuit (IC) as a waveform generator (Intersil, 2009). The oscillator circuit operates with an external capacitor and resistors as shown in figure 3.4

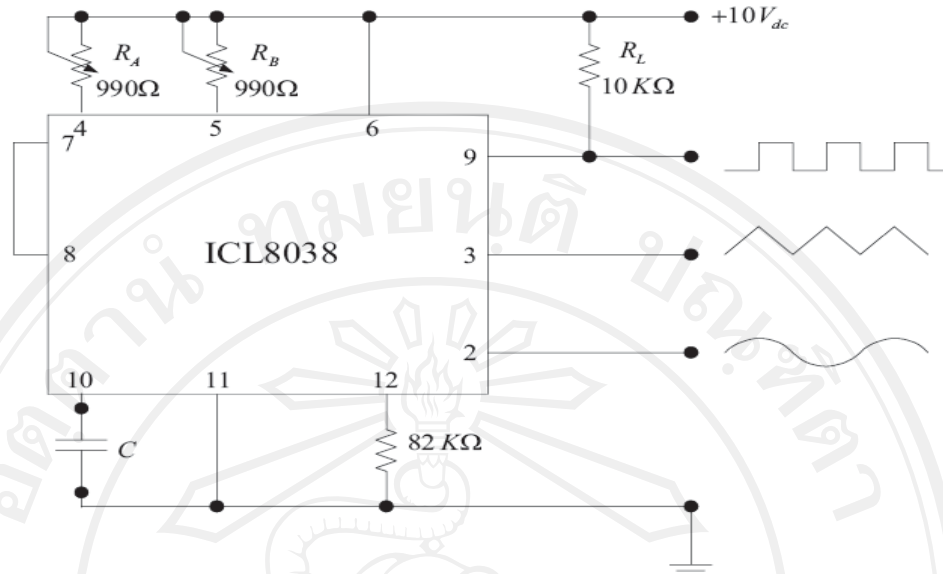


**Figure 3.4 ICL8038-based oscillator circuit**

The signals can be generated using an ICL8038 IC by setting the values of the external components. There are three main components of the oscillator circuit, i.e.,  $R_A$ ,  $R_B$  and  $C$ . A generated signal frequency depends on the waveform timings. We can adjust the frequency by setting the values of the timing resistors  $R_A$  and  $R_B$ . The resistor  $R_A$  controls the timing of the rising portion of triangle and sine waves. For a square wave,  $R_A$  controls the timing of state 1. The time interval of the triangle wave and sine wave rising portion (or state 1 of a square wave) can be computed from

$$t_1 = \frac{CV}{I} = \frac{\frac{1}{3}CV_{\text{supply}}R_A}{0.22V_{\text{supply}}} = \frac{R_A C}{0.66} \quad (3.8)$$

The time interval of the waveform falling portion of the triangle wave and sine wave (state 0 of the square wave) can be computed from

$$t_2 = \frac{CV}{I} = \frac{\frac{1}{3}CV_{\text{supply}}}{2(0.22)\frac{V_{\text{supply}}}{R_B} - (0.22)\frac{V_{\text{supply}}}{R_A}} = \frac{R_A R_B C}{0.66(2R_A - R_B)} \quad (3.9)$$

The wave from frequency is given by

$$f = \frac{1}{t_1 + t_2} = \frac{1}{\frac{R_A C}{0.66} \left[ 1 + \frac{R_B}{2R_A - R_B} \right]} \quad (3.10)$$

Thus a 50% duty cycle can be achieved by setting  $R_A = R_B$ . If we set  $R_A = R_B = R$ , then the frequency can be computed from

$$f = \frac{0.33}{RC} \quad (3.11)$$

### 3.1.6 Dried longan aril-based capacitor

The principal idea of the design is to use dried longan aril as dielectric material inserted between parallel plates of an external capacitor in the oscillator circuit. Dried longan aril were packed in a cylindrical plastic container with a diameter of 25 millimeters and a length of 14 millimeters with a connecting lead attached to both sides of the cylinder as shown in figure 3.5. This dried longan aril-based capacitor was connected to the oscillator circuit as shown in figure 3.6.



Figure 3.5 Proposed dried longan aril-based capacitor

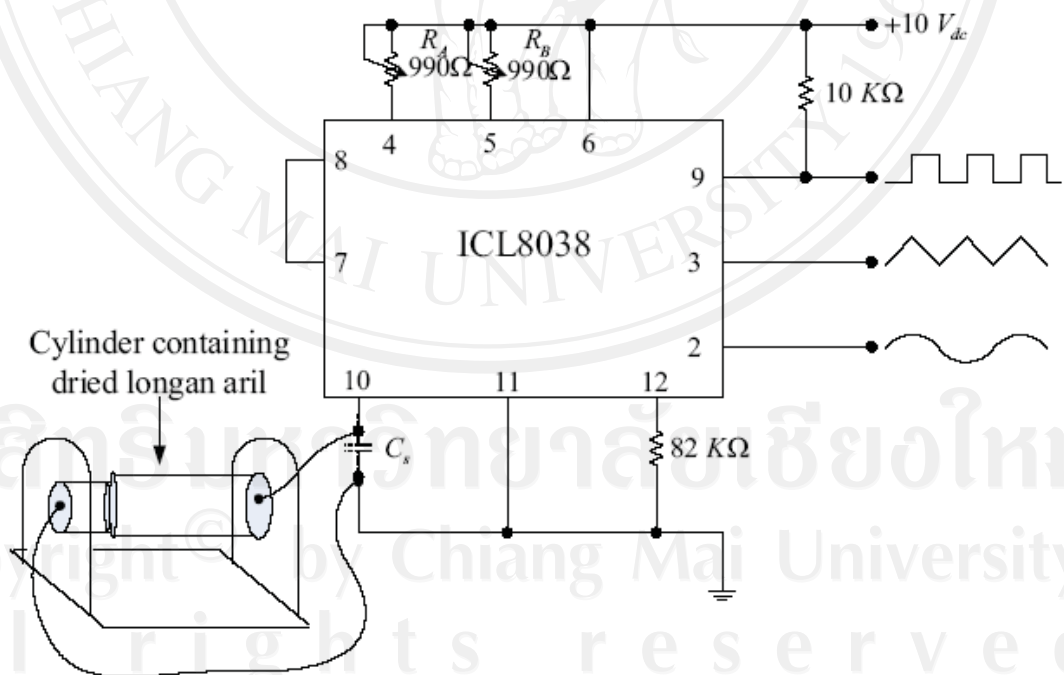


Figure 3.6 Oscillator circuit using dried longan aril as dielectric material



Before connecting the cylinder containing dried longan aril to the circuit, we measured the stray capacitance in the system by generating a pulse signal without a capacitor connected. The duty cycle of the oscillator circuit was set to 50% by setting two variable resistors to 990 ohms. The frequency of the pulse signal was read by a PIC16F877 microprocessor. This frequency was compared with that yielded by an oscilloscope to make sure that the microprocessor yielded a correct frequency. From the experiments, we found that the microprocessor worked properly. Without a capacitor connected, the frequency of the oscillator circuit output was measured 1014.7 kHz. From equation (3.11), the stray capacitance was approximately 328.50 picofarads. When the cylinder containing dried longan aril is connected to the system, it acts as a capacitor in parallel connection to the stray capacitor  $C_s$ . Therefore, equation (11) is accordingly modified to

$$f = \frac{0.33}{R(C_s + C_l)} \quad (3.12)$$

where  $C_l$  is the capacitance of the longan-based capacitor that we would like to estimate.

### 3.1.7 Frequency divider circuit

A PIC16F877 microprocessor was designed to read a signal frequency below 50 kHz. Because the oscillator circuit generated signals with frequency much more than this specification, a divider circuit was applied to divide the generated frequency by 32 as shown in figure 3.7. Two 74LS14 inverters were used to shape the input waveform to a near perfect pulse waveform. Two 74LS93 4-bit counters divided the input frequency by 32 and yielded the output frequency of about 31.71 kHz.

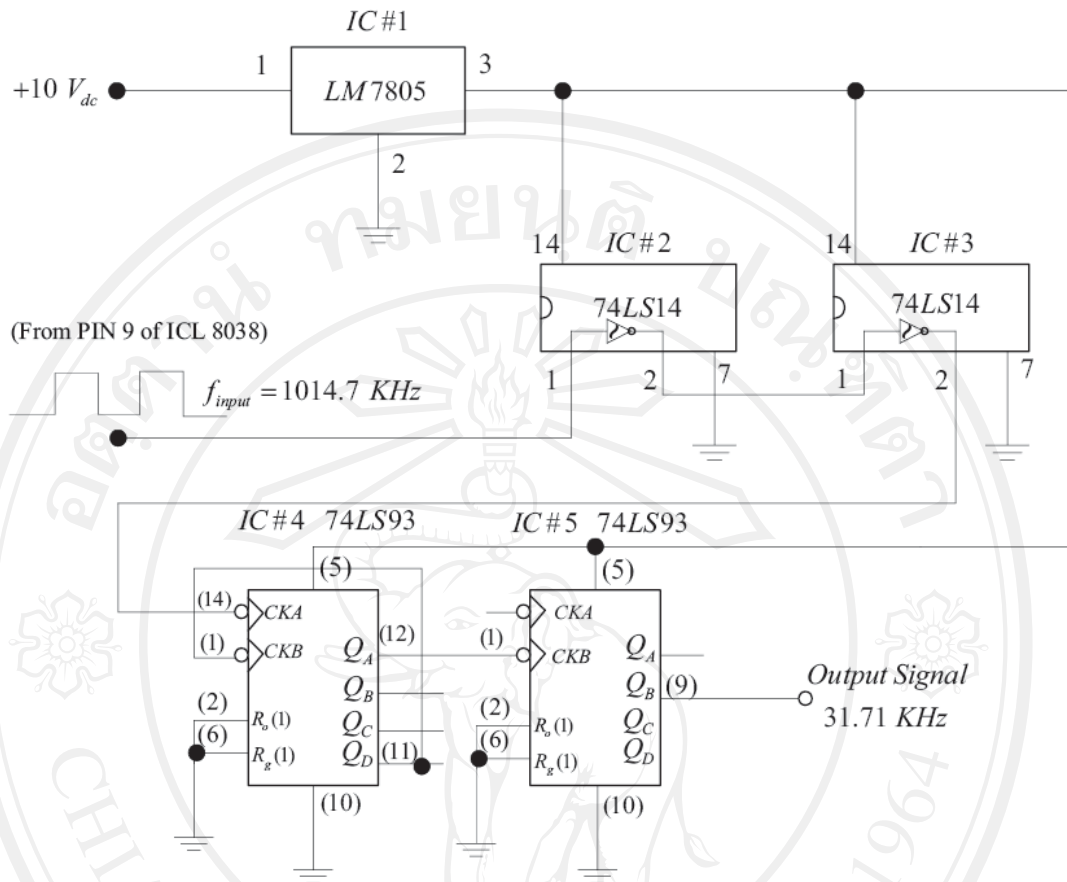
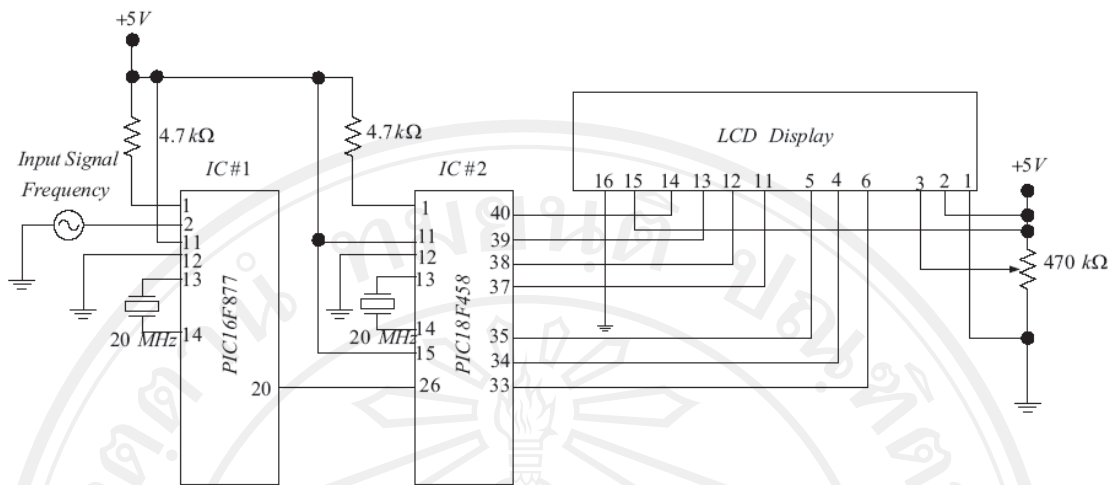


Figure 3.7 Frequency divider circuit

### 3.1.8 Processing and display circuit

As mentioned in the previous section, a PIC16F877 microprocessor was used to read the frequency of the pulses generated by the oscillator circuit. The frequency information was sent to a PIC18F458 microprocessor for further processing. The PIC18F458 microprocessor computed the capacitance of the longan-based capacitor using equation (3.12). It also computed the dielectric constant and the moisture content of dried longan aril in the cylinder. Moreover, it was applied to display the derived information to users via a 4-line LCD. The circuit diagram of the processing and display unit is depicted in figure 3.8



**Figure 3.8 Processing and display circuit of the moisture measurement system**

The real prototype moisture measurement system for dried longan aril is shown in figure 3.9. The dried longan aril-based capacitor was connected from outside the system box via a cable. The LCD was set to display the moisture content and the dielectric constant of the sample inside the cylinder as shown in figure 3.10 and 3.11.

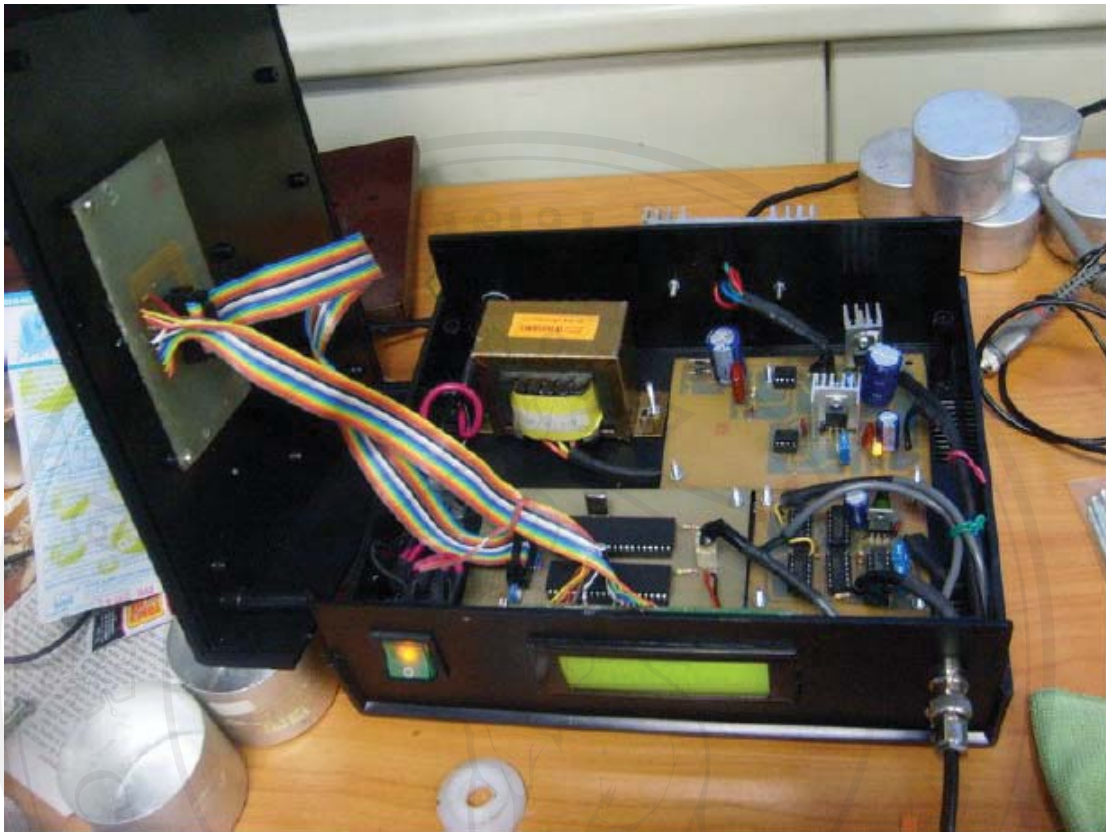


Figure 3.9 Inside the real prototype moisture measurement system



Figure 3.10 Information of moisture content and dielectric constant shown on LCD



Figure 3.11 Prototype of moisture meter

## 3.2 Experimental setup

### 3.2.1 Dried longan aril preparation

Based on the conventional drying process, longan fruits cv. Daw were dried at 70°C for 13 hours, and subsequently at 75°C for 20 hours. The temperature was later maintained at 65°C for another 10 hours or until the moisture content was decreased to 10% Wb. The samples were withdrawn on a two-hour basis after the drying process was initiated for 25 hours. The moisture content of samples were performed at 70°C under vacuum condition for 8 hours or until there was no change in dry weight as shown in Figure 3.15. Figure 3.12 and 3.13 indicate the process of longan drying and the difference in moisture content of longan. The employed drying process and subsequent analyses were in accordance with the official methods and recommended

practices of Association of Official Analytical Chemists (AOAC, 2005). The actual moisture content in each sample was estimated by

$$\text{Moisture content} = \frac{\text{Weight before drying} - \text{Weight after drying}}{\text{Weight before drying}} \times 100\% \quad (3.13)$$

The preparation of dried longan samples is summarized in the following steps:

(1) At the beginning of drying process, 500 longan aril samples were dried in a hot air oven.

(2) From the experiments, we can predict the moisture content of dried longan at any given drying time (see figure 4.2). Therefore, 100 samples with 25 % Wb can be withdrawn at 35 hours after the beginning of drying process. The samples were kept in a vacuum bag to protect the moisture.

(3) Other 100 samples with 22 % Wb can be withdrawn at 38 hours after the beginning of drying process. The samples were kept in a vacuum bag to protect the moisture.

(4) Other 100 samples with 18 % Wb can be withdrawn at 43 hours after the beginning of drying process. The samples were kept in a vacuum bag to protect the moisture.

(5) Other 100 samples with 14 % Wb can be withdrawn at 48 hours after the beginning of drying process. The samples were kept in a vacuum bag to protect the moisture.

(6) The remaining 100 samples with 10 % Wb can be withdrawn at 55 hours after the beginning of drying process. The samples were kept in a vacuum bag to protect the moisture.



**Figure 3.12** Longan drying process: moisture content was estimated by hot air oven

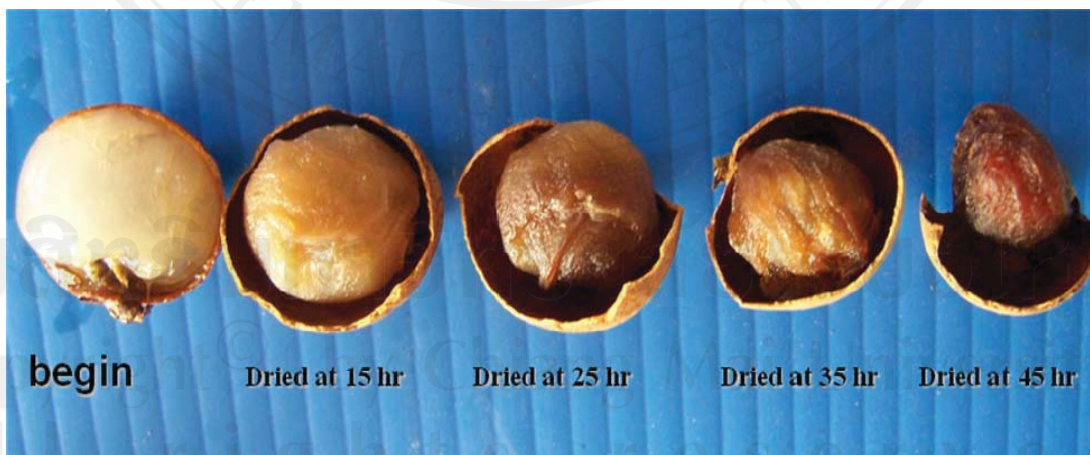


**Figure 3.13** Longan drying process: the initial moisture content of 75% Wb was decreased to 13.5% Wb

The electrical capacitance of longan aril was measured by the proposed moisture measurement system. The aril was placed between two stainless steel discs

inside a cylindrical plastic container. The weights of aril were varied from 9, 10, and 11 grams which were equivalent to the bulk densities of 1300, 1450, and 1600 kg/m<sup>3</sup>, respectively. Figure 3.14 indicates the experimental setup of dried longan in the moisture measurement system.



**Figure 3.14** Experimental setup for dried longan aril moisture content measurement system.



**Figure 3.15** Actual moisture content dried at 70 °C under vacuum for about 8 hours or until their weights are constants.



To investigate the water activity ( $a_w$ ) of the dried longan aril, ten samples of each 10, 14, 18, 22, and 25 %Wb moisture contents were tested. The information from these 50 samples was used to study the relationship between moisture content and water activity ( $a_w$ ).

### 3.2.2 Blind testing

Five different moisture contents of 10, 14, 18, 22, and 25 % Wb and three bulk densities of 1300, 1450, and 1600 kg/m<sup>3</sup> were considered. For each of the five moisture contents and each of the three bulk densities, 100 samples of dried longan aril were tested. Therefore, the total of 1500 samples were tested. The information from these 1500 samples was used to create the relationship among the dielectric constant, bulk density, and moisture content of dried longan aril in the system. In addition, to verify that our proposed moisture measurement system works in general, we performed the blind testing experiments on 47 samples of dried longan aril with 7 different moisture contents. By blind testing means the longan aril samples being tested were not used in any step of the system creation. The numbers of samples are 9, 5, 4, 7, 9, 6, and 7 for 11, 12, 13, 14, 15, 16 and 18 % Wb moisture contents, respectively.

### 3.2.3 Evaluation measures

The measurement procedure employed in the current study was a comparison between the unknown and the standard values. There might exist errors which were caused by associated equipments or an operator. The operator who recorded the value might not be well aware of the measurement principle or how to properly operate the equipment. It was thus possible that the obtained value might differ from the true value in varied extent, or in other words, the measurement errors might exist.

#### 3.2.3.1 Absolute error

The absolute error could be estimated from expected and measured values which could be expressed in percentage as indicated in equation (3.14).

$$e = Y_n - X_n \quad (3.14)$$

When

$e$  = Absolute error

$Y_n$  = Expected value

$X_n$  = Measured value

$$\text{Percent error} = \frac{\text{Absolute error}}{\text{Expected value}} \times 100\% \quad (3.15)$$

or

$$\text{Percent error} = \frac{e}{Y_n} \times 100\% \quad (3.16)$$

Substituting  $e$  with the value from equation (3.14) yields

$$\text{Percent error} = \left| \frac{Y_n - X_n}{Y_n} \right| \times 100\% \quad (3.17)$$

### 3.2.3.2 Accuracy

Accuracy is the closeness between the expected and measured values. The closer of the two values, the higher accuracy. The highest value of accuracy could not exceed unity. The accuracy could be calculated by using equation (3.18).

$$A = 1 - \left| \frac{Y_n - X_n}{Y_n} \right| \times 100\% \quad (3.18)$$

Percentage of accuracy could be calculated by

$$a = 100\% - \text{Percent error} \quad (3.19)$$

or

$$a = A \times 100 \quad (3.20)$$

where

$A$  = Accuracy

$a$  = Percentage of accuracy

$Y_n$  = Expected value

$X_n$  = Measured value

### 3.2.3.3 Precision

Precision is the measurement of closeness between each measured value of one variable and the average of every measured value. The precision could be calculated by equation (3.21).

$$\text{Precision} = 1 - \left| \frac{X_n - \overline{X_n}}{\overline{X_n}} \right| \quad (3.21)$$

$\overline{X_n}$  could be calculated from

$$\overline{X_n} = \frac{\sum x}{n} = \frac{x_1 + x_2 + x_3 + \dots + x_n}{n} \quad (3.22)$$

Where

$X_n$  = number of measurement  $n$  times

$\overline{X_n}$  = average of measurement  $n$  times

## 3.3 Moisture content prediction model based on multilayer perceptrons and support vector regression

Artificial neural networks and support vector regression are well-described in literatures (Vapnik, 2000; Christiani and Taylor, 2000; Haykin, 2009). We provide only their brief introduction in this research.

### 3.3.1 Artificial neural network

An Artificial Neural Network (ANN) is a mathematical model mimicking the biological neural network. An ANN can be considered as a universal function approximator and has been applied to several areas of research such as military, medicine, business. The typical structure of a feed forward neural network is displayed in figure 3.16. The goal is to find the best set of weights ( $\mathbf{w}$ ) so that the

outputs  $o_{j,n}$  are as close to the desired outputs  $d_{j,n}$  as possible for a given input pattern  $x_{i,n}$ ,  $i = 1, \dots, P$  and  $j = 1, \dots, Q$ .  $P$  and  $Q$  are the number of input features and the number of classes, respectively.

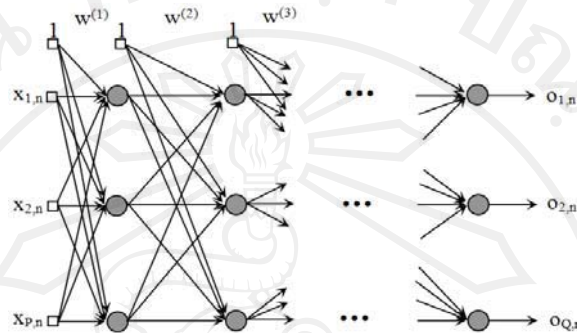


**Figure 3.16 Feed forward neural network.**

### 3.3.2 Support vector regression

In the support vector regression, the goal is to find a function  $f(\mathbf{x})$  that has an  $\varepsilon$ -deviation from the actually obtained target  $y_i$  for all training set,  $\{\mathbf{x}_i, y_i\}$ ,  $\mathbf{x}_i \in \mathcal{R}^n$ ,  $y_i \in \mathcal{R}$  with  $l$  observations. At the same time,  $f(\mathbf{x})$  is as flat as possible. Suppose  $f(\mathbf{x})$  takes the following form:

$$f(\mathbf{x}) = \langle \mathbf{w} \bullet \mathbf{x} \rangle + b \quad (3.23)$$

Where:

$\mathbf{w}$  = A weight vector

$\mathbf{x}$  = An input vector

$\langle \bullet \rangle$  = The dot product

$b$  = A bias

Therefore, the objective is to choose a hyperplane that minimizes the Euclidean norm vector  $\|\mathbf{w}\|$  while simultaneously minimizes the sum of the distances from the data points to the hyperplane. By introducing  $2n$  Lagrange multipliers  $\alpha$ ,  $\alpha^*$

and using the Karush-Kuhn-Tucker (KKT) theory (Christiani and Taylor, 2000). We obtain:

$$\mathbf{w} = \sum_{i=1}^l (\alpha_i - \alpha_i^*) \mathbf{x}_i \quad (3.24)$$

Substituting equation 3.24 into equation 3.23 yields the regression function:

$$f(\mathbf{x}) = \sum_{i=1}^l (\alpha_i - \alpha_i^*) \langle \mathbf{x}_i \bullet \mathbf{x} \rangle + b \quad (3.25)$$

where,  $\mathbf{x}_i$  are the support vectors predetermined by the training patterns. From the KKT conditions, the support vectors are only the points  $\mathbf{x}_i$  where exactly one of the Lagrange multipliers is greater than zero. For the nonlinear case, the input data need to be mapped into a high dimensional feature space. Let the nonlinear transformation function be  $\Phi(\bullet)$  and using the kernel functions defined as:

$$K(\mathbf{x}_i, \mathbf{x}) = \langle \Phi(\mathbf{x}_i) \bullet \Phi(\mathbf{x}) \rangle \quad (3.26)$$

This implies that the dot product in the high dimensional space is equivalent to a kernel function of the input space. There are many types of kernel functions that can be used. The bias term  $b$  may be dropped if it is contained within a kernel function and the regression function in equation 3.25 is given by:

$$f(\mathbf{x}) = \sum_{i=1}^l (\alpha_i - \alpha_i^*) K(\mathbf{x}_i, \mathbf{x}) \quad (3.27)$$

$$f(\mathbf{x}) = \sum_{i=1}^l \beta_i K(\mathbf{x}_i, \mathbf{x}) \quad (3.28)$$

### 3.3.3 Moisture content prediction models

In this research, the input to the regression models is the dielectric constant of dried longan aril whereas the output is the moisture content. There are no parameters to set for the linear and polynomial regression models. However, there are some parameters to set for the MLP and SVR. For the MLP, back-propagation algorithm was applied in the training phase. Therefore, we needed to find the best structure for this particular problem, i.e., the number of hidden layers and the number of neurons in each hidden layer. For the SVR, the  $\varepsilon$ -insensitive loss function was applied. The support vectors are on the two hyper-planes with  $\varepsilon$  distance from the real hyper-plane. Therefore,  $\varepsilon$  is an error between an actual hyper-plane and the support vector hyper-planes. The data standing between the support vector hyper-planes are considered to produce no error. In the training stage, we try to find the support vector hyper-planes that can cover all training data. That is, all training data must be in between the two support vector hyper-planes.

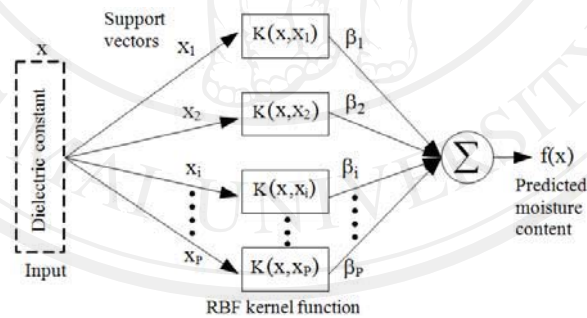
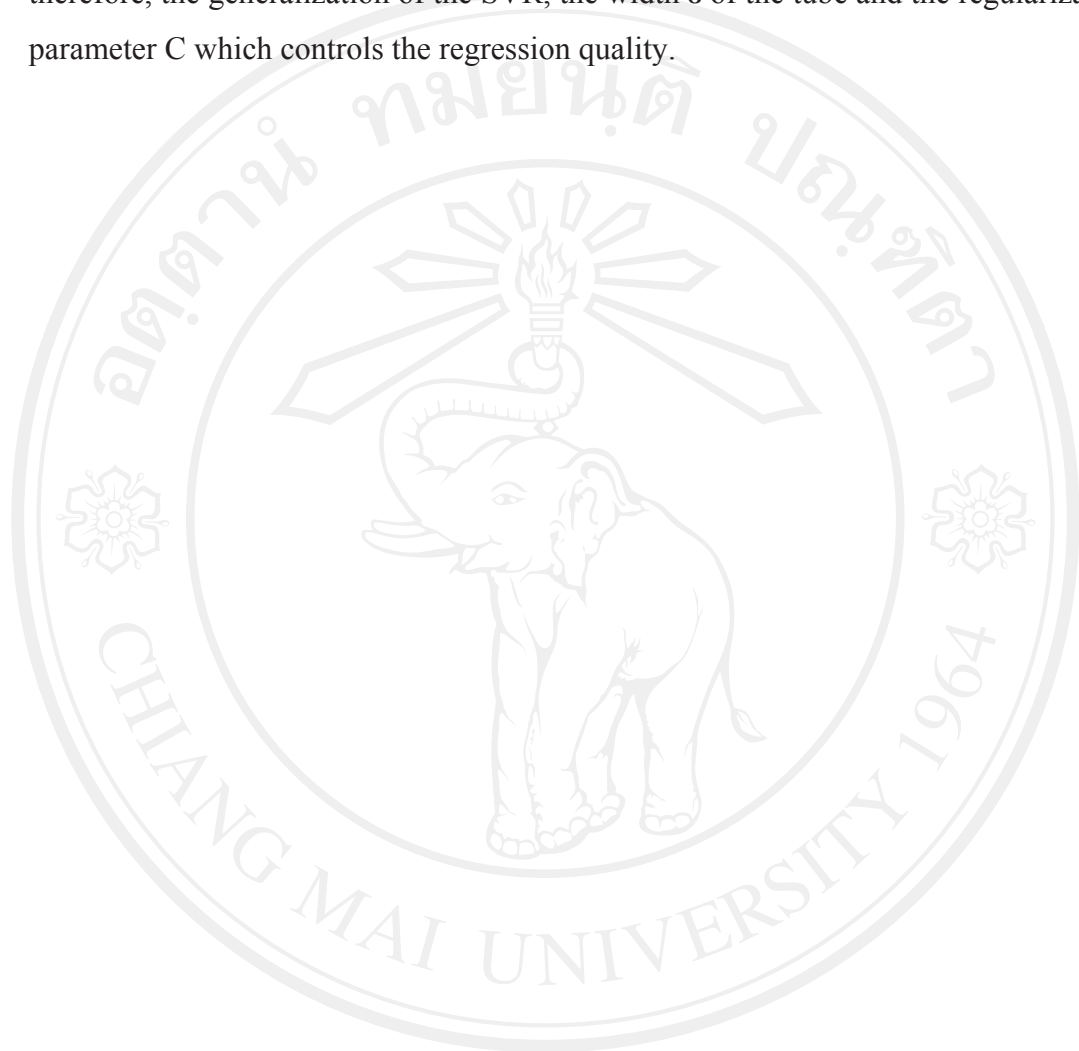


**Figure 3.17 Architecture of SVR-based moisture content prediction model.**

Figure 3.17 shows the architecture of the prediction model. In this study, the Radial Basis Function (RBF):

$$K(\mathbf{x}_i, \mathbf{x}) = \exp\left(-\|\mathbf{x}_i - \mathbf{x}\|^2 / 2\sigma^2\right) \quad (3.29)$$

was used as the kernel function. Some important parameters to set for the SVR model include the RBF kernel specific parameter  $\sigma$  that controls the spread of the RBF and, therefore, the generalization of the SVR, the width  $\varepsilon$  of the tube and the regularization parameter  $C$  which controls the regression quality.



ลิขสิทธิ์มหาวิทยาลัยเชียงใหม่  
Copyright© by Chiang Mai University  
All rights reserved